REPORT OF GROUP VII

HADRON AND PHOTON EXPERIMENTS AT FIXED-TARGET ACCELERATORS

Convenor : Yu.D.Prokoshkin

A.N.Diddens, R.Diebold, J.-M.Gaillard, Yu.V.Galaktionov,
S.S.Gerstein, J.Pilcher and R.Sosnowski.

ABSTRACT

Possible hadron and photon experiments at 20 TeV stationary-target proton accelerator have been considered in order to see typical limitations and possibilities of the experiments in this new energy domain.

1. INTRODUCTION

The aim of our study is to analyze typical hadron and photon experiments which could be performed at the stationary-target Very Big Accelerator (VBA) with proton beam energy of 20 TeV. We have covered the following experimental topics:

- "standard" hadronic experiments,
- hadroproduction of particles with new flavours,
- muon pair production,
- high-p_T experiments,
- experiments with hyperons and
- photon-beam experiments.

Our approach in this study was the following:

i) we tried to define the experimental limitations, as well as new possibilities, on the basis of the present-day knowledge and experiments;

ii) for our selected topics, we made a kind of preliminary design of the experimental set-ups in order to see what do experiments look like;

iii) besides, we compared the possibilities of the experiments at VBA with those of the pp, $p\bar{p}$, ep and e^+e^--colliders, that might exist by this time (1999).

Before starting the discussion of actual VBA experiments we would like to remind the reader that VBA is the fixed-target proton accelerator with the accepted energy of 20 TeV. Its circumference is 75 km. The typical hadron beam at this accelerator is about 3 km long. Due to the huge center-of-mass γ-factor the experimental set-ups will have "one-dimensional" geometry: 1 km is needed typically in the forward direction, and only 1 m laterally. The angle of diffraction scattering will be as small as 10 microradians (1 cm over 1 km); 90° in the center of mass corresponds to 10 mrad in the laboratory.

For designing the VBA experiments the numerical information is needed, as an input: beam intensity, spatial resolution in detectors, field in magnets, etc. We adopted that in

1999 the following characteristics could be achieved:

- external proton beam average intensity will be $3 \cdot 10^{12}$ per sec for a 10 sec spill (this corresponds to the limit of $3 \cdot 10^{14}$ protons per pulse, given in Section III of this Workshop);
- spatial resolution in charged particle detectors will be 20 micron regularly and even 5 micron in special cases (see Section VIII);
- magnetic field in the standard spectrometric magnets will be 8 to 10 Tesla.

2. EXAMPLES OF HADRONIC EXPERIMENTS

We will consider first the "classical" experiments which are to be performed at any proton accelerator, entering a new energy domain: total cross-sections, elastic scattering, scaling in particle production, search for new particles, etc.

2.1 Elastic Scattering

Let us start with the elastic scattering of $\pi^{\pm}$, $K^{\pm}$, p and $\bar{p}$. Although pp and $p\bar{p}$ elastic scattering will have been studied at even higher center-of-mass energy $\sqrt{s}$ by this time,using colliders, still it will be of interest to see the energy variation for $\pi^{\pm}p$ and $K^{\pm}p$ elastic scattering and how it relates to the rise in the total cross-sections. Further, all six particles can be scattered off the neutron in a liquid deuterium target, and with the very high luminosity pp elastic scattering can be followed down many decades.

The first step is to form a secondary beam and to identify the beam particles. As was shown in last year's study[1)], such beams are straightforward, typically scaling in length with momentum p as $\sqrt{p}$. $\sigma_p/p \sim 10^{-5}$ ($\pm$200 MeV/c at p = 20 TeV/c) is easily achieved.

Using three synchrotron-radiation detectors (Ar, Xe and NaI) sensitive to X-rays of different energies, Willis found[1)] that π/K/p separation could be achieved over the range 3 to 50 TeV (see also Section VIII).

Next we consider a magnetic spectrometer for the forward scattered particle (fig. 1). We emphasize that this is not an optimized system, but rather an existence proof that elas-

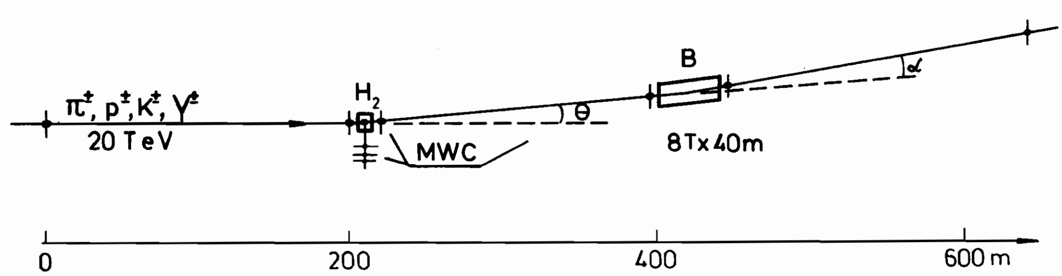

Fig. 1. A typical spectrometer for the study of the elastic scattering at 20 TeV. H_2 is a liquid hydrogen target. B is 40 meter long 8 Tesla superconducting magnet. Here as well as in the next figures, we denote the high-accuracy track detectors by MWC ("Multi-wire-chamber"-type).

tic scattering is relatively easy to measure at these energies. If we take $\sigma_x = \pm 20$ micron resolution for the chambers measuring the coordinates, then

$$\sigma_\theta = \sigma_\alpha = \frac{2\sigma_x}{L} = \frac{2\text{x}20 \text{ micron}}{200 \text{ meter}} = \pm 0.2 \text{ microrad.} \quad (1)$$

This gives $\sigma_{p_T} = \pm 4$ MeV/c at p = 20 TeV/c. Multiple scattering in a 30 cm liquid hydrogen target gives ± 3 MeV/c, so that the total p_T-resolution is

$$\sigma_{p_T} = \pm 5 \text{ MeV/c}, \quad (2)$$

good enough even for the Coulomb region ($p_T \leqslant 50$ MeV/c). With the magnet aperture of 5 cm the acceptance is $\Delta\theta = 0.2$ mrad, $\Delta p_T = 4$ GeV/c at 20 TeV/c.

Assuming a 40 m bend of 8T (magnet B in fig. 1), the bend angle at 20 TeV/c is $\alpha =$ = 5 mrad, and $\sigma_p/p = \sigma_\alpha/\alpha = 0.2$ microrad/5 mrad, so

$$\sigma_p/p = \pm 4\cdot 10^{-5}, \quad \sigma_p = \pm 0.8 \text{ GeV/c}. \quad (3)$$

While this is not enough to isolate elastic scattering by itself, the resolution is comparable to that in a background-free FNAL experiment which also looked at the recoil proton.

Since the recoil kinematics are quite similar at different energies, the experiment here will look much like the two-arm elastic experiments at present energies. In particular, any pion produced must carry away less than a few σ_p of energy, say $E_\pi \lesssim 2$ GeV in laboratory system, and simply measuring the recoil direction will give strong discrimination against the inelastic reactions.

Special care must be taken to detect the recoil in the Coulomb-interference region. A gas target such as used in recent Serpukhov, CERN and FNAL experiments should be adequate.

Elastic scattering of the neutron will require a neutron detector with good spatial and energy resolution (Hodoscope hadron calorimeters, see Section VIII).

For hyperon elastic scattering one might make the forward magnetic spectrometer shorter, especially at lower energy. As shown below (§ 5), a rather clean Σ^- beam can be achieved with momenta above 15 TeV/c. This beam has a decay path of 600 m, and even with the long spectrometer of fig. 1 about one third of the Σ^- would survive.

2.2 Total cross-sections

The nature of the rise of hadron total cross-sections, which first manifested itself in the "Serpukhov effect", has no theoretical explanations until now. So, it is important to study how are the total cross-sections rising with energy for hadrons with different quark structure. To answer this question precise measurements at VBA are needed.

This is again a simple extrapolation of experiments at present energies. One could use the standard transmission counter technique or the elastic scattering spectrometer(fig. 1), centered at $\theta = 0$, although its precision is far more than required. A 2-meter long liquid-hydrogen target would give an attenuation of the beam by a factor of 0.7 for a 40 mb total cross-section and multiple scattering would give a transverse momentum kick of ±10 MeV/c to the beam.

To allow the extrapolation to $\theta = 0$ one could use fast matrix logic with the beam spectrometer wire chambers to record events having small angle scatters (p_T = 60 to 300 MeV/c, $|t|$ = 0.004 to 0.1 $(\mathrm{GeV/c})^2$). The magnetic bend in the spectrometer could be utilized to limit this extrapolation to elastic and near-elastic scatters.

The accuracy in total cross-section determination as high as 0.2% can be achieved without problems. This is an order of magnitude better than with pp and $p\bar{p}$-colliders.

A deuterium target would also be used in order to measure total cross-sections on neutrons. Similar information from heavier targets would have physics interest in this energy region (rising cross-sections) and would give also the "engineering" information required to determine absorptive corrections in other hadronic experiments.

Again, total cross-sections for hyperons could be easily measured with a shorter apparatus.

2.3 Inclusive reactions

It would be very interesting to check the scaling in the inclusive particle production processes using various secondary beams. According to the field-theoretical approach a breaking of the cross-section scaling is expected for the central (pionization) region. Also, there are some cosmic-ray indications of scaling violation above 10 TeV even in the fragmentation region, Feynman $x > 0.2$.

The study of the inclusive x-distributions at large x for various combinations of beam and target particles will show also how the quark-counting rules ($(1-x)^n$) are fulfilled at very high energies.

Reactions of the sort

$$\pi^- + p \to \pi^- + \ldots \tag{4}$$

at large x could be easily studied with a simple set-up like in fig. 1. Although one could identify π^- in the spectrometer with the synchrotron radiation, other processes such as

$$\pi^- + p \to K^- + \ldots \tag{5}$$

with a fast K^- will have much lower cross-sections and will not present much background to the first reaction.

Exchange reactions, such as (5), will be much more difficult to see due to the background from (4), and further studies of synchrotron-radiation particle identification are needed.

Particles produced at $90°$ in the center of mass with $p_T \gg m$ will have a laboratory angle of $1/\gamma_{CM} \approx 10$ mrad for a 20 TeV beam. The laboratory momentum would then be $p_{lab} \approx 100 p_T$. Separation of π/K/p will be difficult at $p_T \gtrsim 3$ GeV/c. π^0, η, K_S and Λ would all give a clean signature, however.

Particles emitted more backward in the center of mass would be easier to identify with Cerenkov counters.

2.4 New particle searches

The center-of-mass energy for a 20 TeV proton beam incident on a nucleon at rest is $\sqrt{s} = 0.2$ TeV. This is much less than will have been available from $p\bar{p}$ colliding beams ($\sqrt{s} = 2$ TeV at FNAL Tevatron and 6 TeV at UNK, Serpukhov) for some years before 20 TeV VBA machine. However, the fixed-target accelerator will have the advantage of much higher (10^7!) luminosity: $\mathcal{L} \approx 4 \cdot 10^{37}$ cm^{-2} sec^{-1} for $2 \cdot 10^{12}$ interacting protons per sec. This is five orders of magnitude beyond even a pp-collider such as ISABELLE. Thus, VBA could discover very rarely produced particles of mass $M \lesssim 100$ GeV/c^2.

2.4.1 Monopoles

One could look for these objects as they fly out of an interaction, e.g. by their intensive Cerenkov radiation. Alternatively, one could autopsy a beam dump to look for monopoles deposited over a long period of time. The integrated luminosity achieved over one year of running would be enormous:

$$\mathcal{L} \sim 10^{45} \text{ cm}^{-2}/\text{year}. \tag{6}$$

2.4.2 Quarks

Here one would tune a secondary beam to a "supermomentum" (like in early experiments at Serpukhov), say, 24 TeV/c for ordinary, charge-one particles, but only p = 8 TeV/c for q = 1/3 quarks. This would correspond to x = 0.4 for light quarks and $x \approx 0$ for M = 80 GeV/c^2 quarks. With a negative beam one could go to somewhat lower momenta before being overwhelmed by π^- and Σ^-.

2.4.3 Heavy penetrating particles

One could form a beam out of the forward particles coming from a beam dump. For example, particles produced at rest in the center of mass would have $\gamma = 100$, and the laboratory momentum of a M = 30 GeV/c^2 object would be p = 3 TeV/c. The thickness of the beam dump would be adjusted to keep the flux to $\lesssim 10^6$ particles/sec, so that background could be kept to a low level. Then Cerenkov counters could be used to reject muons and to measure the masses of these particles ($\gamma = 100$ is easy for gas differential Cerenkov counters).

By keeping the beam dump reasonably thin, the experiment would be sensitive to particles with absorption cross-section as large as a few millibarns. For example, a 5 m iron dump would be 25(35) absorption lengths for pions (protons), but only 2.5 absorption lengths for particles with 1 mb/nucleon absorption cross-section. This would give a factor-of-ten loss of such particles. The multiple scattering in 5 meters of iron gives $\sigma_{p_T} = \pm 350$ MeV/c, less than might be expected from the production mechanism.

2.4.4 Heavy long-lived particles

This is similar to the last two searches, except that now one wants to be sensitive to strongly interacting particles of charge $q = \pm 1$. Again a secondary beam is formed, and Cerenkov counters are set to give sensitivity in the region $\gamma \lesssim 10^3$. Special emphasis is given to $\gamma \approx 100$ to pick up particles produced near rest in the center of mass. One would then sweep out the mass range by running for few days at each of several momenta.

For total beam flux of 10^6/sec (mainly $\pi^\pm$ and protons) this would give an upper limit of one heavy particle per 10^{11} light ones. With a beam of 1 km length and a life-time of 10^{-8} sec, only 5% of the $\gamma = 100$ particles would survive. The short-lived particle beam of length 100 m, described below in §5, would push the life-time limit to 10^{-9} sec for heavy particles, produced with $x \approx 0$, and to correspondingly shorter life-times for lighter particles with higher γ.

3. HADRONIC PRODUCTION OF NEW FLAVOURS

Secondaries are produced with high-energy stationary-target accelerator with much larger γ-factor, and their decay vertex can be separated from production point much easier than for colliding beam machines. This enables us to obtain a nearly background-free sample of decays of particles, providing their life-time is $\tau \gtrsim 10^{14}$ sec, just the case of hadrons with new flavours (charm, beauty ...).

3.1 Decay properties and production dynamics

One might expect beauty-hadrons to decay with $\tau = 10^{-14}$–10^{-13} sec. This corresponds to the average decay length of 1 to 10 cm for a 10 TeV particle with the mass of $M = 5$ GeV/c^2 (table 1).

For hadrons, containing top-quark (if it exists), the estimation of τ is less reliable. However, even if they decay rapidly ($\tau < 10^{-14}$ sec), top-hadrons may be recognized since their decay products contain quite often beauty-hadrons ($t \to b \to \ldots$ is the main decay channel). The observation of a beauty-hadron decay vertex would enhance the signal-to-background ratio for parent top-hadrons.

The recent data on charmed hadron production at the ISR energies indicate that the central production contributes to this process less than expected. Other mechanisms giving particles in the fragmentation region seem to be important. Similar situation might be expected for b- and t-hadron production. In order to understand the production dynamics, experimental data on new flavour hadron distributions and flavour-antiflavour correlations are needed.

Table 1

Hadroproduction of 10 TeV particles, containing c,b,t quarks

Quark	Mass of particle [GeV/c^2]	Life-time [sec]	Decay length [cm]	Production cross-section [microbarn]
c	2	$3\cdot 10^{-13}$	45	200
b	5	10^{-13}	6	10
	5	10^{-14}	0.6	10
t	16	$\ll 10^{-14}$	$\ll 0.2$	1

At the ISR energies, $\sqrt{s} \sim 50$ GeV, recent experiments suggest that charmed hadrons are produced with a cross-section of the order of 0.1-0.2 millibarn. Taking into account the mass difference of c- and b-quarks one can estimate the production cross-section for the b-hadrons at 20 TeV as ~10 microbarn. With the beam of $5\cdot 10^5$ protons one b-hadron would be produced in a target 0.01 absorption length thick.

Due to the strong angular collimation of secondaries, produced at a stationary target, the geometrical acceptance of a vertex detector is close to 100%. Of course, not all decay modes are equally easily observed. The reduction factor of 0.1-0.01 has to be taken into account.

3.2 Experimental possibilities

Existing detectors such as high-resolution bubble and streamer chambers and high-preasure drift chambers enable us to see the decay vertex of charmed particle. Scaling up the length of these detectors with the energy of the investigated particles (fig. 2) we keep constant the possibility to separate the production and decay vertices (both the decay length and the error of vertex determination, in the beam direction, are $\sim$ E).

Beauty-hadrons are expected to be heavier than charmed particles. One would then expect that the lower limit of the life-time at which the decay point can be distinguished from the production vertex will be larger for beauty-hadrons(the decay length is $\sim 1/M$).

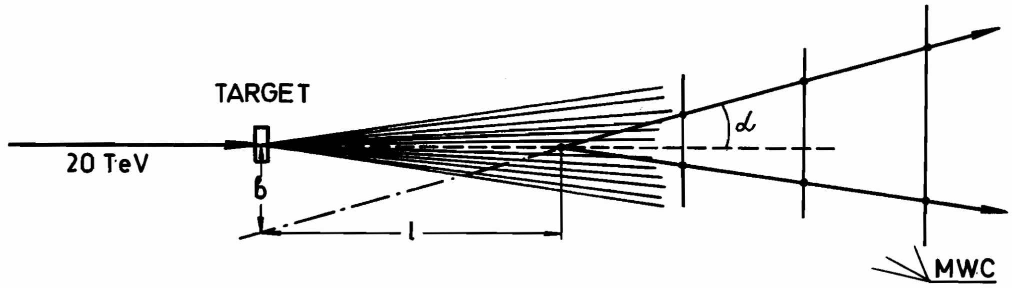

Fig. 2. The scheme of the new-flavour production experiment. Note the scaling: $\ell \sim E$, $\delta a \sim 1/E$, $\delta b = \ell \delta a$ = const.

However, the precision of the localization of the decay vertex increases with M. As a consequence the lower limit of the life-time of beauty-hadrons at which we can distinguish a decay vertex will be about the same as that for charmed hadrons.

One might expect that eventual progress in the detector technique will lower the present limits of the accessible decays to $\lesssim 10^{-14}$ sec at the VBA time (5 micron accuracy in detectors defining the vertex).

Finally, let us consider the experiments, which are not scaled, but which are becoming possible only above 10 TeV, where the decay lengths are 1 meter. The scheme of such an experiment is shown on fig. 3. The intense Σ^- beam (§5) is directed onto the tungsten target-dump, ~1.5 meter thick. The target serves as a strong absorber for ordinary hadrons (~15 abs. lengths). As for the new-flavour hadrons, some of them have much smaller absorption cross-section, $\sigma_{abs} \lesssim 10$ mb. The typical examples are F-meson, with (cs) quark structure, and (csd)°-baryon (which could be recognized via its characteristic decay into Ξ^-+...) As the result of different absorption the secondary flux could be strongly enriched by new-flavour particles.

4. MUON PAIR PRODUCTION

There are several important reasons for studying lepton pair production up to the highest possible masses, using the fixed-target accelerators.

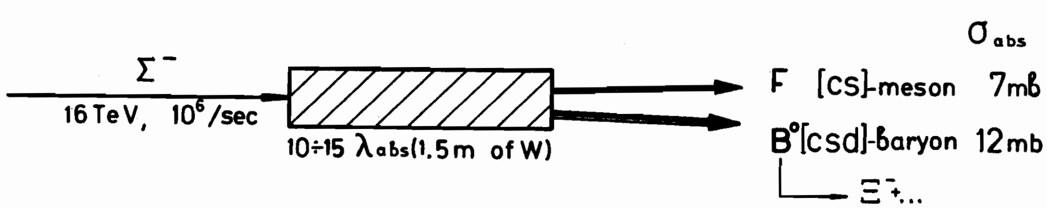

Fig. 3. The scheme of the enrichment of new-flavour flux using the difference in the absorption (see text).

4.1 Structure functions and QCD

It is fairly well established that lepton pair production, for values of $M/\sqrt{s} \simeq 0.05$, proceeds through quark-antiquark annihilation. Thus the cross-section reflects the quark distribution functions of the interacting hadrons. In nucleon-nucleon interactions lepton-pair production provides a measurement of the sea quark distribution in the nucleon. For unstable, or rare particles like π, K, $\bar{p}$,Σ it provides practically the only way to measure the energy distribution of the constituents.

Many of these structure functions have, or will have been measured with lower energy machines. One of the important contributions of VBA is the measurement of structure functions at far higher $Q^2(M^2)$ values.

QCD predicts how these functions should evolve with Q^2. The new measurements will test these predictions. One striking result would be a departure from the QCD-behaviour at high Q^2 if the theory were incorrect or if, for example, the quarks had a substructure. The pair of 100 GeV mass probes distances of

$$L_0 \approx 2 \cdot 10^{-16} \text{ cm.} \qquad (7)$$

Lepton pair production at large p_T is thought to be due to QCD processes rather than the electromagnetic annihilation of on-shell quarks as at low p_T. Thus high-p_T pair production can be used to isolate these effects. The kinematically available p_T range at a 20 TeV machine is expanded by factor 7 compared to existing fixed-target accelerators.

4.2 Heavy $q\bar{q}$ bound states

The $c\bar{c}$ and $b\bar{b}$ bound states have both been discovered in lepton-pair production. At least one more new quark is expected and its mass appears to lie above the current generation of e^+e^- machines. Still other quarks may well exist.

In searching for new flavour bound states, pair production experiments offer a broad mass acceptance, high resolution and very high luminosity. For example, a lepton pair experiment using 10^{12} interacting protons per second from VBA sees an effective luminosity of $2 \cdot 10^{37}$ $cm^{-2}sec^{-1}$, 10^5 higher than that of ISABELLE-like pp-colliders.

4.3 Weak-electromagnetic interference

As is shown below, lepton pair experiment with 20 TeV machine would see a very strong intermediate Z^o-boson signal as well as a large event rate from the nearby mass continuum. Substantial interference effects are expected between the resonance and the continuum.

This interference manifests itself as an asymmetry between the μ^+ and μ^- momentum distributions. The effect is large at muon pair masses $M_{\mu\mu} \gtrsim 40$ GeV/c^2, the asymmetry is expected to be higher than 50%. The study of this phenomenon would provide measurements of the quark-Z^o coupling constants.

4.4 Cross-sections and event rates

Lepton pair production studies at the existing machines have found that the production cross-section by protons scales with incident energy as

$$d\sigma/dM_{\mu\mu} = f(\tau)/M^3_{\mu\mu} \tag{8}$$

where $\tau = M^2_{\mu\mu}/s$. Present data[2)] is well described by

$$f(\tau) = 8\cdot 10^{-33}\exp(-\tau/0.035)\ \mathrm{cm^2 GeV^2}. \tag{9}$$

We used these relations to obtain the cross-section (fig. 4) for 0.4 TeV (SPS), 3 TeV (UNK) and 20 TeV (VBA) stationary-target machines. Also shown is the cross-section for pp-collider of 0.4+0.4 TeV (ISABELLE).

The cross-section of 20 TeV protons is lower compared to an ISABELLE-like machine.But it is much more than compensated by the higher luminosity (10^5) out to masses over 100 GeV/c^2. In fig. 4 we introduced this luminosity factor in the cross-section in order to compare directly the counting rates of VBA and ISABELLE.

A unique feature of the fixed-target accelerator is the ability to produce high-energy secondary beams. Pions are especially interesting for lepton pair production since they carry a fast valence antiquark. A pion beam of 7.5 TeV/c with $>10^{10}$ pions/sec can be produced with VBA proton beam. The expected muon pair production cross-section for these pions is shown in fig. 4. It is an application of the fit to the present data of

$$d\sigma/dM_{\mu\mu} = 3.5\cdot 10^{-32}\exp(-\tau/0.066)/M^3_{\mu\mu}\ \mathrm{cm^2\ GeV^2}. \tag{10}$$

Again we introduced a factor of 10^{-3} to compensate for the difference in the luminosities.

In the Salam-Weinberg theory the Z^o has a mass of ≈ 90 GeV and a partial width to muon pairs ~ 80 MeV[3)]. The production cross-section times muon-pair branching ratio (3%) is expected to be $\sim 2\cdot 10^3$ times larger than the continuum cross-section per GeV, at the same mass (fig. 4).

The asymmetry between the μ^+ and μ^- momentum spectra,

$$A = \frac{\sigma(p_- > p_+) - \sigma(p_- < p_+)}{\sigma(p_- > p_+) + \sigma(p_- < p_+)} \tag{11}$$

which is the result of the weak-electromagnetic interference, is shown on fig. 5. It was calculated by J.Rutherfoord using papers[4,5)]. Here $p_-(p_+)$ is $\mu^-(\mu^+)$ momentum. As it is seen from the figure, the event rate in the mass region of $M_{\mu\mu} \approx 50$ GeV/c^2, where the asymmetry (11) has a maximum value,is large enough to study the interference.

4.5 Experimental set-up

Fig. 6 shows a possible detector for high sensitivity muon-pair studies. It is modelled after the CFSW-detector of E-605, FNAL. The beam is targeted at the upstream end of 30 m

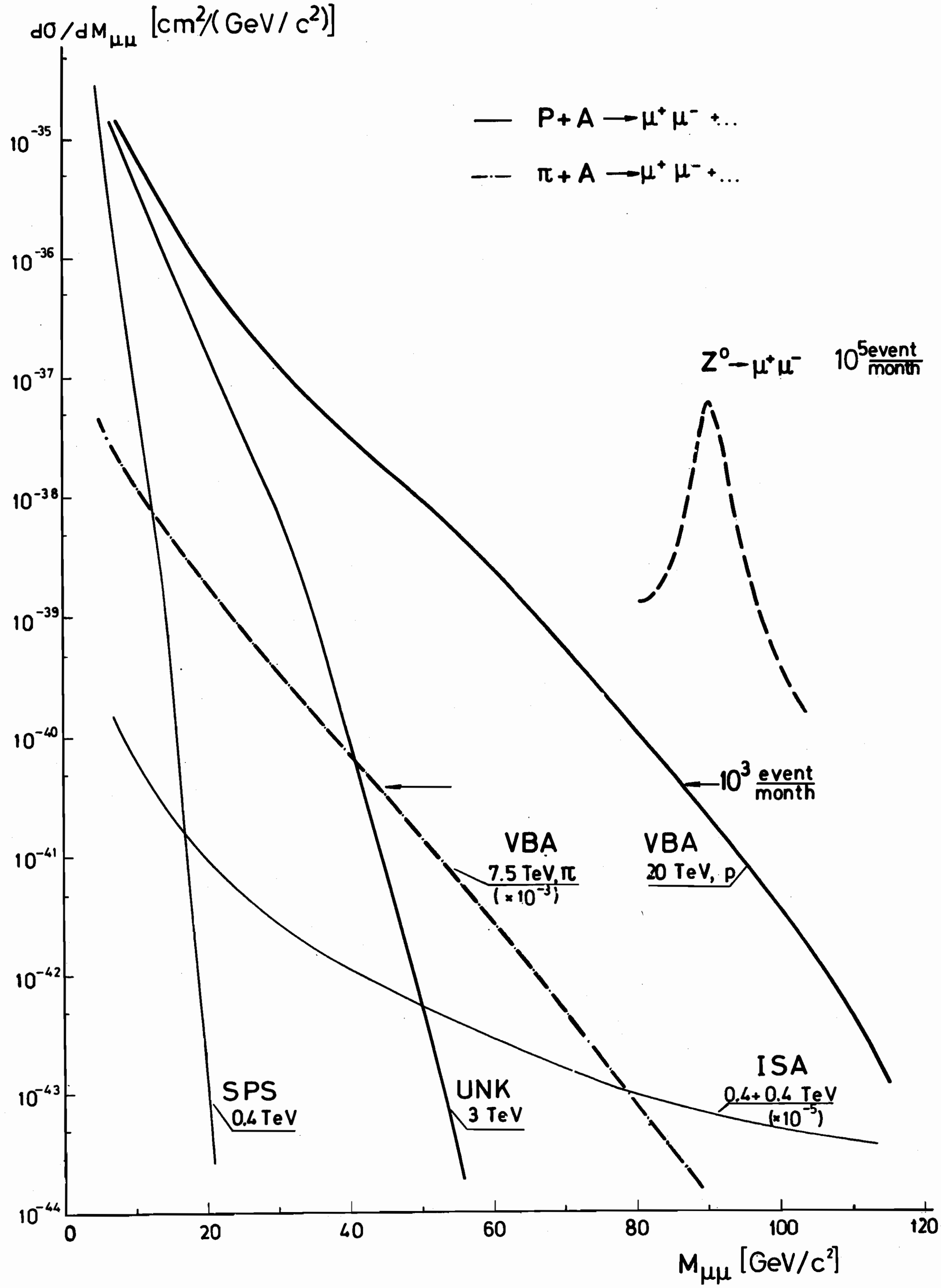

Fig. 4. Muon-pair production cross-sections and event rates.

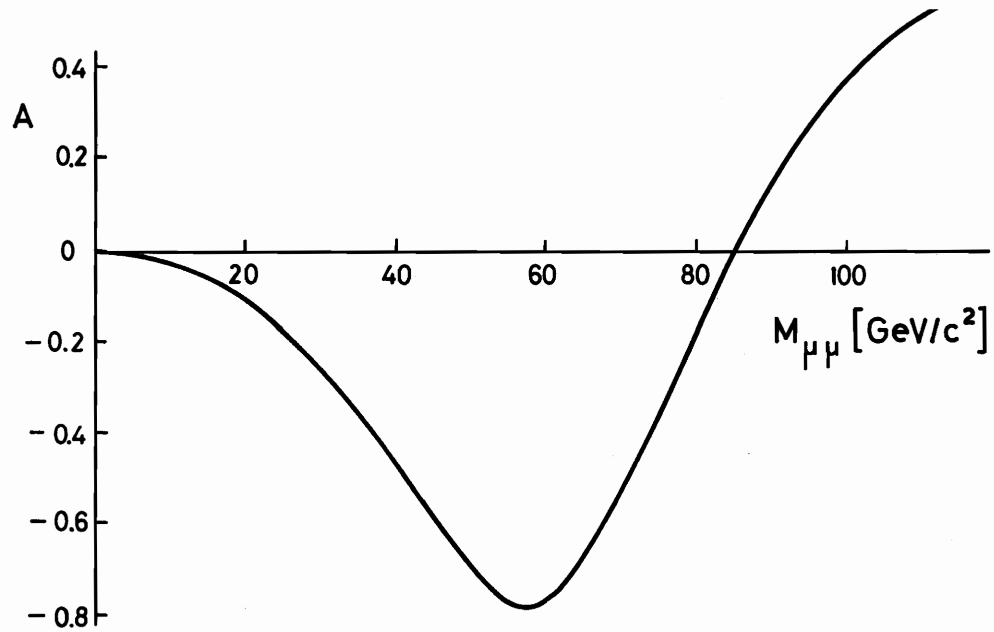

Fig. 5. The asymmetry between muon spectra (11) due to the weak-electromagnetic interference.

long conventional dipole B_1. A cooled dump is located in the forward direction to absorb the non-interacting beam; 25 meter long dump should be adequate to reduce the secondary particle flux to a tolerable level. The magnetic field of B_1 and B_2 magnets further reduces charged particle background. Beryllium can be added to the acceptance regions of the magnet to help further.

Magnet B_2 is a superconducting dipole, 30 meter long, with a field up to 5 T. The purpose of B_1 and B_2 is to bend parallel the muon pairs in the mass range of interest.

The pairs are detected downstream in the spectrometer built around dipole B_3. This is taken as a conventional magnet with 1.8 T field. The detector planes (MWC) before and after B_3 are taken to have moderate (in the scale of 1999), 100 micron resolution. This should lead to a mass resolution of

$$\Delta M_{\mu\mu} / M_{\mu\mu} \approx 1\% .$$

At the downstream end of the detector there are some iron shields each 1-2 meter thick, for final muon tagging.

The above detector would provide the counting rate of ~100 muon pairs per GeV per month at $M_{\mu\mu} \sim 100$ GeV/c^2, produced by 20 TeV protons (fig. 4) while 10^6 $Z^\circ \to \mu^+\mu^-$ events could be collected in a one-year experiment.

4.6 Muon-pair production by hyperons

Pion and kaon beams of 10^6/sec have been used successfully to study the quark distributions within these hadrons. At VBA a Σ^- beam of such an intensity will be available (see

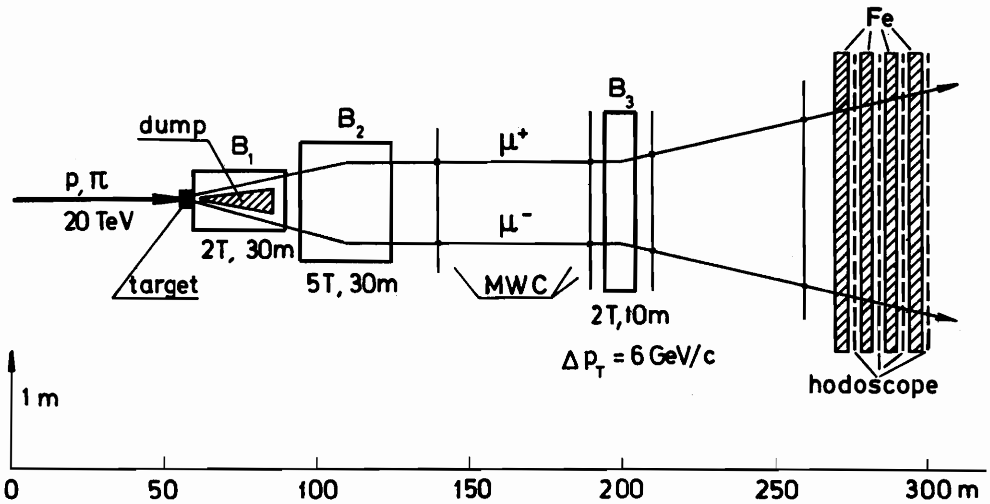

Fig. 6. The set-up for muon-pair production experiment.

§5), so a similar study could be envisaged for this hyperon.

Muon pairs from Σ^--nucleon interactions would be produced by $s\bar{s}$ and $d\bar{d}$ annihilation for x of the Σ^- quark beyond the sea region. A measurement of $d^2\sigma/dM_{\mu\mu}dx$ leads to the determination of the quark distribution[6]. We note that in this case the s and d quark distributions are not separated.

For the experiment with a Σ^- beam a large acceptance spectrometer could be used similar to that in fig. 6, but somewhat shorter.

5. HIGH-p_T SCATTERING

The hard-scattering models predict that at energies of 20 TeV the high-p_T hadron scattering ($p_T \geqslant 10$ GeV/c) will be governed by the asymptotic QCD. The inclusive production of jets, hadrons or single photons at 90° in the center of mass should follow p_T^{-4} dependence:

$$E\frac{d^3\sigma}{dp^3}(A+B\to C+\dots)\sim\frac{1}{p_T^4}F\left(x_T=\frac{2p_T}{\sqrt{s}}\right). \tag{12}$$

5.1 Jets

Jet production at high p_T can be used as one of the most direct tests of QCD predictions since the quark and gluon fragmentation functions, which are inputs for QCD calculations, are bypassed. By observing jet-jet correlations one should be able to measure the quark transverse momentum distribution in hadrons.

At presently available energies jets are difficult to observe, but in the VBA experiments the jet selection should not be a problem. This type of physics will be covered partly by colliders, but only for pp and $p\bar{p}$ cases, not for other particles, and in a limited p_T range

(10^5-10^7 difference in luminosities).

5.2 Production of hadrons at large p_T

High-p_T hadron production becomes the direct QCD test at VBA since constituent interchange contributions (p_T^{-n} in CIM, n = 6,8,12) which are important at present energies, should die out at 20 TeV, $p_T \gtrsim 10$ GeV/c. Thus, one is left with only low-order QCD diagrams of quark-quark and gluon-quark scatterings. Using the data from high-p_T jet production one can isolate quark (and gluon) fragmentation functions. For QCD-test the ratios of cross-sections obtained with different beam and target particles (A and B) or different final states (C) should be even more reliable since any scaling violations, if present, tend to cancel in ratios.

5.3 Direct high-p_T photons

Direct photon production at high p_T is especially interesting since the photon has a point-like coupling to a quark. Photon can thus participate directly in the gluon-quark scattering

$$gq \to \gamma q \,, \tag{13}$$

or in the "bremsstrahlung" process

$$gq \to gq\gamma, \tag{14}$$

both giving p_T^{-4} dependence. Reaction (13) has a unique signature. It has a high-p_T direct photon unaccompanied by hadrons as it is usually the case for high-p_T π^o production. The direct photon nearly always has a quark jet on the opposite side, not a gluon jet. Thus, triggering on single high-p_T photons one can study the features of accompanying quark jet.

5.4 Cross-sections and rates

As an example we give in fig. 7 the invariant cross-sections for two inclusive high-p_T reactions of (12)-type: direct-photon production

$$\pi^+ + p \to \gamma_{dir} + \cdots \tag{15}$$

and pion production

$$\pi^+ + p \to \pi^o + \ldots \tag{16}$$

both at 90° in the center of mass. These are the QCD predictions[7]. The jet production cross-sections are typically 10^3 times higher.

The event rate shown on fig. 7 was estimated for luminosity $\mathcal{L} = 3\cdot10^{37}$ cm^{-2}/day (10^9 incident π^+ per accelerator cycle, 5 meter long liquid-hydrogen target). One sees that p_T values as high as 50 GeV/c are accessible at VBA.

5.5 Experimental set-up

Fig. 8 shows a possible realization of a high-p_T scattering experiment. The general features of the experiment are the following.

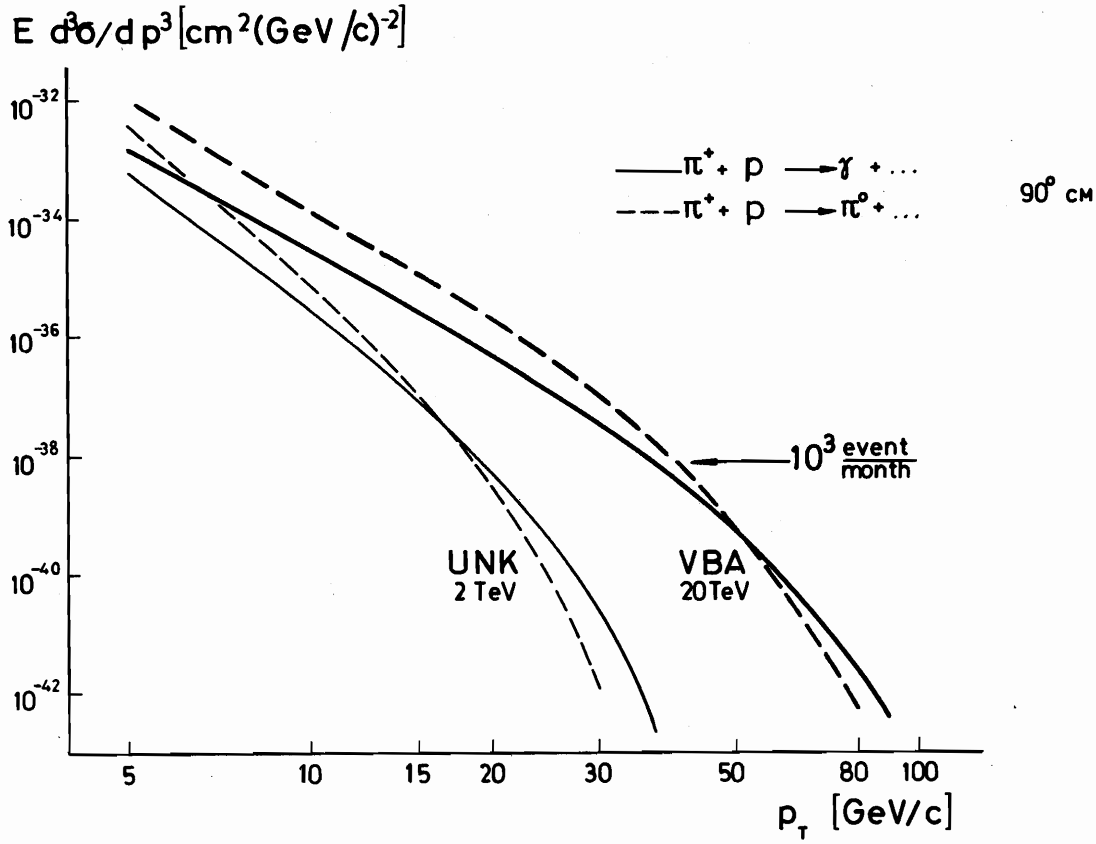

Fig. 7. Single γ and π^0 production cross-sections at high p_T.

For high-p_T events the particle multiplicities in jets are typically 10, the angular size of the jet being 0.1-0.5 mrad. A typical laboratory energy for high p_T, say 30 GeV/c, is 30 GeV x (γ_{CM} = 100) = 3 TeV.

To keep the geometrical event pattern (to disentangle jets) one should abandon magnetic fields. Individual charged particle identification is not possible, as a rule, although one might identify π^0, K_S, Λ, γ through their decay or using the difference in the electromagnetic and hadronic shower development in the detector.

The set-up is basically a combination of hodoscope calorimeters which allow a simultaneous measurement, with high accuracy, of photon and hadron energies and coordinates (see Ref. 8 and Section VIII for detailed description of these detectors). It is preceded by the coordinate-measuring detectors (MWC). To avoid the overlap of hadron showers coming from two jets (separated by some mrad) the distance from the target to the hodoscope calorimeter should be $\gtrsim$ 200 m.

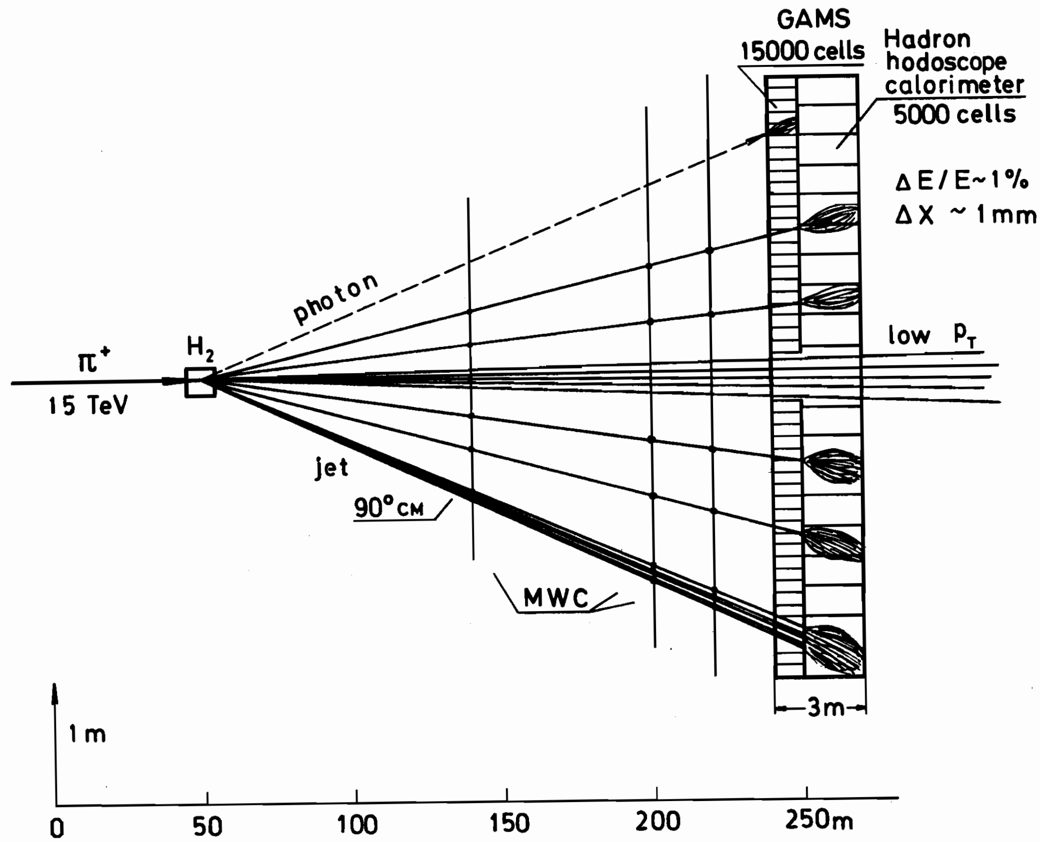

Fig. 8. Experimental set-up for high-p_T studies. GAMS is the hodoscope lead-glass gamma-spectrometer with 4x4 cm^2 cells. Hadron hodoscope calorimeter is built of 10x10 cm^2 cells.

High-p_T triggers of different kinds could be easily arranged by applying a selection on the radial moment of the cell pulse-heights (see CERN proposal P-110).

6. EXPERIMENTS WITH HYPERONS

As in the existing hyperon beams a point-parallel short-lived particle beam could be realized at VBA, but in much better conditions. The mean decay length of a 15 TeV Σ^- is 600 m, it is 300 m for Ω^-, so a lot of space is available. But to be powerful for a search for short-lived particles also (say, with $\tau \gtrsim 10^{-11}$ sec), the length of this magnetic channel must be kept as short as possible.

6.1 The beam channel

The VBA hyperon beam could be scaled from existing beams. Fig. 9 shows the scheme of hyperon beam produced with 20 TeV protons ($\Delta\Omega = 10^{-8}$ ster., $\Delta p/p \approx 10\%$, beam spot size at target $2 \approx 6$ mm). When one goes from 200 GeV to 20 TeV, the length of the shielding against hadron cascades changes as $\sim \ell nE$, from 10 m to 20 m only.

For protection against the "direct view" of the target 1 $\Delta p_T = 0.8$ GeV/c is needed. Thus, bending power of the channel θ_b is defined by

$$\Delta p_T = \theta_b \times 20\ \text{TeV/c},\quad \theta_b \approx 4\ \text{mrad}. \tag{17}$$

With this bending the hyperon momentum resolution $\Delta p/p \approx 10\%$ could be achieved when the separation between coordinate-measuring detectors (MWC in front of target 2 in fig. 8) is ≈ 50 m.

The necessary secondary beam - primary proton spatial separation (d) defines the distance (ℓ) between the target1 and the shielding in B_2:

$$d\ [\text{mm}] = 0.05\ell^2\ [\text{m}^2] \tag{18}$$

For negative hyperons at 200 GeV d = 7 mm was enough. This leads to ℓ = 12 m at 20 TeV.

For a positive beam the separation from primary protons was achieved mostly by producing secondaries with $p_T > 0.6$ GeV/c. Very little separation can be reached this way at 20 TeV unless ℓ is increased up to 100 m. If one limits the energy of the positive beam to about 8 TeV the separation could be achieved for ℓ = 12 m from the magnetic deflection alone.

The muon background from π and K decays N_μ scales as

$$N_\mu \sim \ell/E. \tag{19}$$

At 20 TeV it is expected to be an order of magnitude lower than at 200 GeV (ℓ = 1.5 m at 200 GeV and 12 m at 20 TeV).

6.2 Fluxes of hyperons and other particles

The fluxes of various particles have been computed by scaling the results from the CERN SPS beam[9] with the measured x-dependence. Fig. 10 shows relative yields of negative particles. Also given are the incoming proton intensities needed for 10^6 beam particles at various x values.

The importance of designing a beam which can transport negative particles up to the

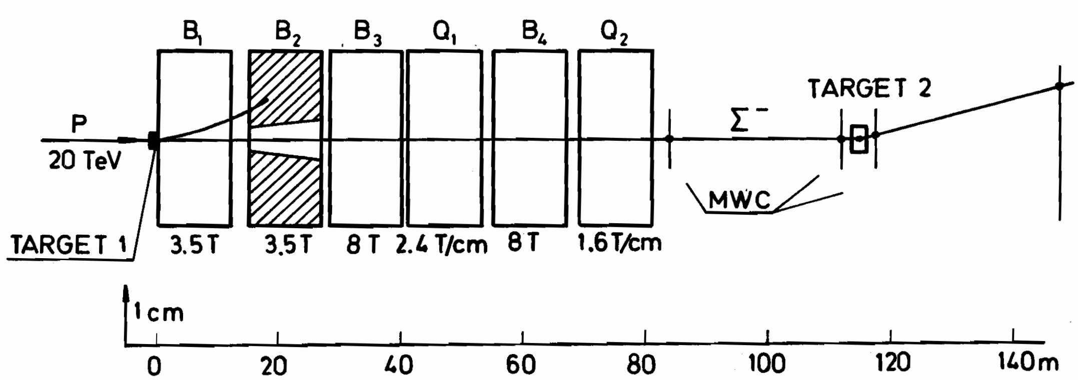

Fig. 9. The scheme of VBA hyperon beam. B_1 and B_2 are 12 m "normal" magnets with θ_b = = 0.6 mrad each. B_3, B_4 are 12 m superconductive magnets, θ_b = 1.4 mrad, Q_1, Q_2 are 12 m quadrupoles.

kinematical limit is obvious from fig. 10. 90% -pure Σ^- beam with $\gtrsim 10^6$ per sec intensity can be obtained at 18 TeV utilizing $3 \cdot 10^{11}$ primary 20 TeV protons per sec.

Other hyperons could also be produced with reasonable intensities ($\sim 10^6 \Sigma^+$/sec, $\sim 10^5 \Xi^-$/sec, $\sim 10^4 \Omega^-$/sec, etc.), but there is a huge problem in their identification in the beam (see Ref. 1 and Section VIII of this Workshop).

6.3 Some possible experiments

Many experiments could be performed with the intense and pure 18 TeV Σ^- beam. Some of them have been discussed above already (elastic scattering, total cross-section, muon pair production). Other interesting applications of hyperon beam are the following.

6.3.1 Diffractive production of new flavour strange baryons

The Σ^- contains already a fast strange quark. To build a strange baryon containing c, b or t quarks only one extra unusual quark is needed. This is an important advantage for the production of these states. The cross-section for the production of charmed strange barions by Σ^- is expected to be ~ 0.1 mbarn.

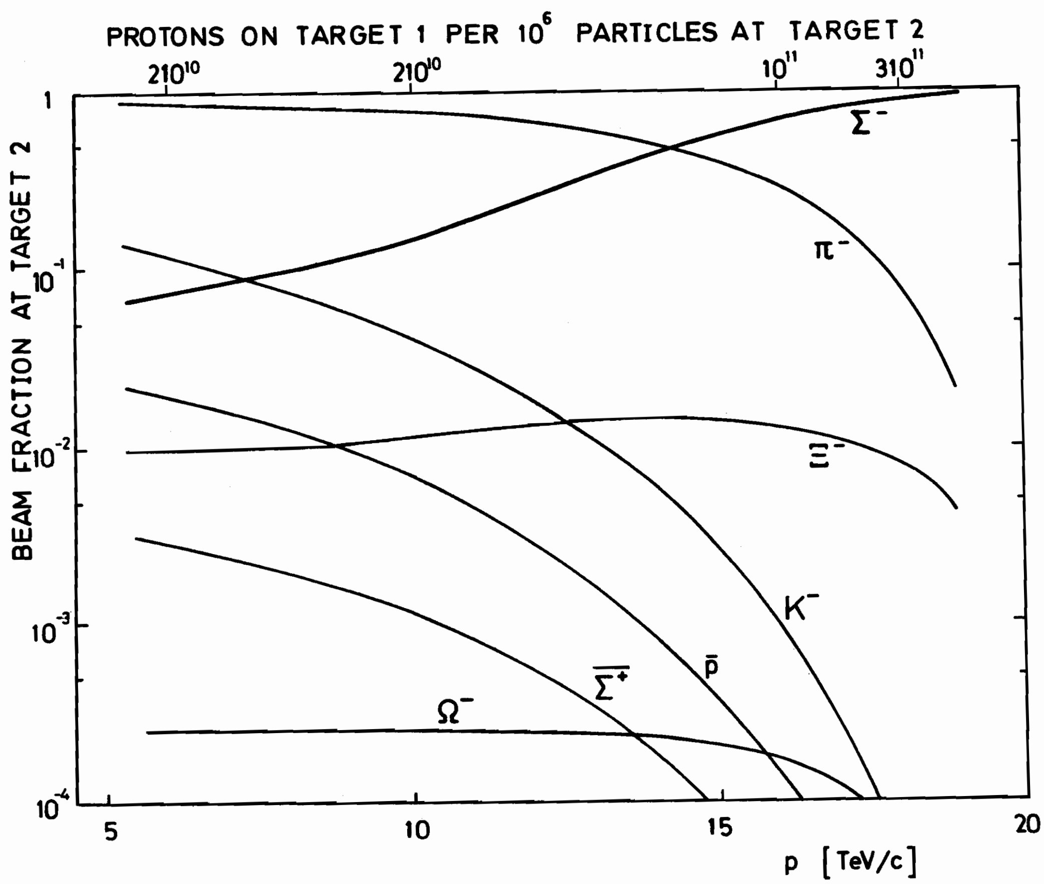

Fig. 10. Fluxes of negative particles in the VBA hyperon beam.

The decay products would include Λ, charged kaons and should be measured by a spectrometer with particle identification. (See also Σ^--dump experiment, § 3).

6.3.2 Σ^- scattering on electrons

For 18 TeV Σ^- scattering on electrons the kinematical limit corresponds to Q^2=18 GeV^2. This is another way to measure various combinations of quark distributions in the Σ^- which may be combined with muon-pair production information (§4) to obtain more specific information on the structure functions.

6.3.3 Ω^- scattering

Should a particle identification scheme be realized in the hyperon beam at a level of 10^{-4} or better one might perform a number of experiments with Ω^-s, studying elastic scattering, total cross-sections, diffractive particle production, etc.

6.3.4 Search for short-lived particles

The beam could be used in the experiments searching for new short-lived particles, with life-time $\tau \gtrsim 10^{-11}$ sec. For the decay loss of 10^3 the limit obtained for the life-time in 15 TeV beam would be

$$\tau\,[\mathrm{sec}] = 2 \cdot 10^{-12}\, M\,[\mathrm{GeV/c^2}] \quad . \tag{20}$$

7. EXPERIMENTS WITH PHOTON BEAMS

7.1 Photon beam

A typical high-intensity, high-purity VBA photon beam is shown on fig. 11. It is scaled from the existing 400 GeV machine beams. Simpler solutions are possible, if the background of neutral hadrons can be tolerated, although this is usually not the case for a somewhat sophisticated experiment.

The four magnets, B_2-B_5, for bending the electrons around the beam-dump, are 2Tx4 m each in the SPS case. The radiation energy losses in the magnets are given by

$$\Delta E/E = 3 \cdot 10^{-13}\, B^2 L p / M^2 \tag{21}$$

where B is in Teslas, p is in GeV/c, magnet-length L is in meters and particle mass M is in GeV/c^2. Scaling such a beam to a 10 TeV photon beam at VBA one might want to keep the same acceptance and momentum resolution and consequently scale the drift-spaces and the L both like $\sqrt{p}$, keeping B constant. The radiation losses of electrons will prevent this, $\Delta E/E$ becoming >1. Fixing $\Delta E/E \ll 1$ one could instead scale the drift-space and L like p, and B like 1/p.

The radiation losses of the electrons might allow a simpler method of producing a pure electron (and then photon) beam. The sweeping magnet in the incident momentum-analysed beam

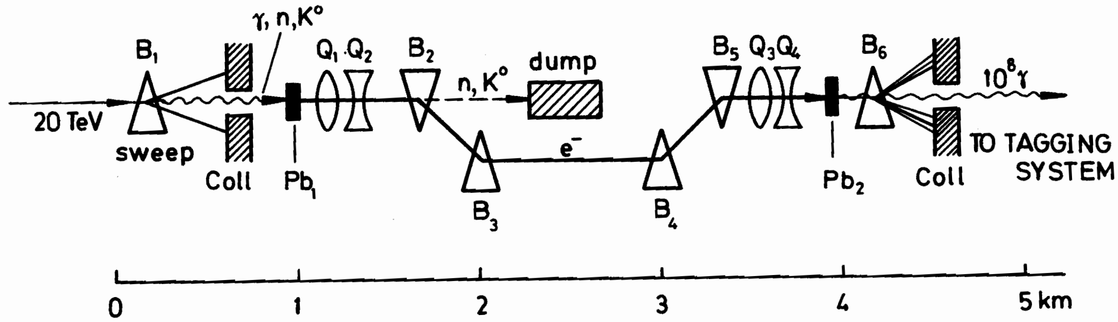

Fig. 11. High-purity, high-intensity VBA photon beam. B_2-B_4 are 0.1 T magnets, 200 m long each.

(fig. 12) can be chosen to give $\Delta E/E = 0.1$, for instance. Then the electrons become separated in space from the other negative beam particles, the radiation losses of which are negligible (21).

In conclusion, no fundamental problems are foreseen, provided one bends the electrons gently. The photon beam will become at VBA some km's long. The same conclusion will hold for the tagging system.

7.2 Fixed-target machine versus ep-collider

Colliders of electrons on protons are being actively studied now. They might be built well before a 20 TeV fixed-target accelerator. An example is 20 GeV e^- on 270 GeV protons[10], with luminosity 10^{32} cm^{-2}sec^{-1}, giving $\sqrt{s} = 150$ GeV. Such a machine is a source of virtual photons with $\nu_{max} = 12$ TeV. This latter figure is similar in energy with VBA photon beam.

One could envisage a tagging system on the collider, selecting low-Q^2 photons, thus simulating real photon beam. For reasonable assumption about the geography of the colliding beam experiment a minimum tagging angle of 10 mrad might be realistic, resulting in $Q^2_{min} \approx$ ≈ 0.1 GeV^2 and a luminosity $\mathcal{L}(\gamma p) \approx 0.01\,\mathcal{L}(ep) = 10^{30}$ cm^{-2}sec^{-1}. This is an order of magnitude of the luminosity of the VBA photon beam traversing a 1 m hydrogen target.

Almost real photons from the above ep-collider will have a laboratory energy in the 10 GeV region, three orders of magnitude lower than at VBA. The fragmentation regions of the

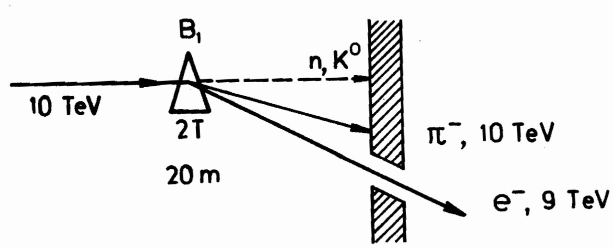

Fig. 12. Scheme of pure e^- beam (for photon beam) realization using the radiation losses.

photons will thus look very different, in energies and in angles, of the two machines.

In a study on ep colliders a number of experiments with low $-Q^2$ photons have been shown to be quite feasible[10]: γp total cross-sections, elastic Compton scattering, diffractive production of vector mesons, deep-inelastic Compton scattering, QCD Compton scattering, QCD Bethe-Heitler and Drell-Yan dimuon production.

7.3. Experiments with the VBA photon beam

The future will tell, whether the competition of an ep-collider will be as fierce as its proponents would make us believe. One might still want to implement at VBA some of the experiments mentioned above, or still have not been done, perhaps because the ep-collider experiments are more difficult to perform than is expected now.

For some types of experiments (few) a high-energy photon beam of VBA might have unique features, not to be found at ep-colliders. We mention two of them.

The photoproduction of relatively long-lived particles, containing c, b, t or other heavy quarks, could be studied with the VBA photon beam. A 10 TeV/c particle of 5 GeV/c^2 mass and 10^{-14} sec life-time has a decay distance of 6 mm. Such a unique signature could be made visible in a streamer chamber or other precise vertex detectors. One might give preference to a photon beam over a charged particle beam because of its much higher efficiency in producing particles containing heavy quarks.

The dependence on atomic number of photon-initiated processes could be studied with the VBA photon beam. This will give the information on the space-time development of final states.

8. CONCLUSION

In the study above we have analysed some directions of the investigations at the 20 TeV VBA. We attempted, by the examples of some real experiments, to make it clear what limitations and what new possibilities arise with this jump in energy of a factor of 50 compared with the existing fixed-target proton accelerators.

We have seen that many hadronic experiments in the range of 20 TeV are obvious extrapolations of the present-day experiments and present no special difficulties. As a rule they require less expenditure (compared with the accelerator cost) than at today accelerators.

The accelerator with a fixed target has the unique feature of providing a rich variety of secondary high-energy particle beams, such as $\pi^{\pm}$, $K^{\pm}$, K^{o}, p, $\bar{p}$, n, $\bar{n}$, Σ^{-}, γ ... (as well as ν and μ). In addition to the beam species, target particles can also be varied (p,n,A). Therefore at VBA one can carry out the investigations of particle interactions in which the possibilities to vary the quark structure of the colliding particles are very wide. This cannot be realized with colliders.

Another important feature of the experiments at VBA is connected with the use of the advantages of ultra-relativistic kinematics. Owing to tremendous γ-factors the decay lengths become much stretched. The production, interaction and decay processes of short-lived particles such as charmed particles, beautiful particles, etc., can be more easily measured. The experiments on hyperon beams as well as the search for new particles seem to be especially attractive.

The main reason for our striving for higher energies is the wish to "touch" deeper the structure of interacting particles and their constituents. If we try to characterize the 20 TeV fixed-target VBA by the value for the energy available in the center of mass ($\sqrt{s}$ = = 0.2 TeV), then it is certainly inferior to the colliders of the near decade (pp -ISABELLE, 0.8 TeV; $p\bar{p}$ - CERN, 0.54 TeV; and also $p\bar{p}$ - Tevatron and $p\bar{p}$ - UNK).

However, one should bear in mind that "touching" deeper the particle structure in such, e.g., classical processes as scattering with large p_T or with the production of high masses in the final state one finds rapidly decreasing cross-sections. Large $\sqrt{s}$ and high luminosity turn out to be both necessary for the experimental investigations of such processes.

Having a luminosity 10^5-10^7 times higher than that of pp and $p\bar{p}$-colliders, VBA is much more powerful for the processes involving masses or transverse momenta up to $\sqrt{s}/2 = 100$ GeV. VBA cannot compete with the pp-colliders in the investigations on muon pair production, when the masses are bigger than 150 GeV. However, here even with the colliding beams we find ourselves in the area where no measurements can be made because the detection rate is no more than one event per month.

The advantages of the 20 TeV machine and pp-colliders must be compared for particular experiments. For instance, VBA provides much higher detection rate for single hadrons with large p_T or Z°s if the mass of the latter ones is 90 GeV. This accelerator is a powerful "Z°-factory" which produces 10^6 $Z^\circ \to \mu\mu$ decays per year. At the same time the production of hadron jets with large p_T is to be studied with pp-colliders. In general 20 TeV fixed-target VBA and pp or $p\bar{p}$-colliders for even higher (in the CM) energies are complementary to each other, but not excluding, for hadron experiments.

VBA provides an excellent photon beam, on which a very interesting program can be realized for 10 TeV range. If high-energy ep-colliders are constructed earlier, they could cover the main part of this program (although cautious people may say, that not a single machine either for high or for low energies has yet been constructed).

The jump to such high energies of hadron and photon beams does not result in great changes in the architecture of experiments. Some limitations connected with the difficulties in particle identification are quite obvious (at least today). At the same time there appear new experimental possibilities connected with the application of calorimeters as basic detectors; with the energy growth they become precise coordinate-energy particle detectors.

* * *

REFERENCES

1) Proceedings of the Workshop on Possibilities and Limitations of Accelerators and Detectors. FNAL, October 15-21, 1978.

2) J.E.Klogan et al. Phys. Rev. Letters 42, 948 (1979).

3) C.Quigg. Rev. Mod. Physics 49, 297 (1977).

4) R.W.Brown et al. Nucl. Phys. B75, 112 (1974).

5) R.F.Peierls et al. Phys. Rev. D16, 1397 (1977).

6) C.B.Newman et al. Phys. Rev. Letters 42, 951 (1979).

7) D.Jones and R.Rückl. Phys. Rev. D20, 232 (1979).

8) Yu.D.Prokoshkin. "Hodoscope calorimeters as basic coordinate-energy detectors of particles in the experiments in the 10 TeV range". Preprint IHEP 79-148, Serpukhov, 1979.

9) M.Bourquin et al. Nucl. Physics B153, 13 (1979).

10) W.Hoogland. Proc. of the Study of an ep facility for Europe. DESY 79/48 (1979).